Jefferson Lab
Thomas Jefferson National Accelerator Facility
Exploring the Nature of Matter

LABORATORY DIRECTED RESEARCH AND DEVELOPMENT PROPOSAL
TITLE: GENERATION AND CHARACTERIZATION OF MAGNETIZED BUNCHED ELECTRON BEAM FROM DC PHOTOGUN FOR JLEIC COOLER

LEAD SCIENTIST OR ENGINEER:	RIAD SULEIMAN AND MATT POELKER
Phone:	(757) 269-7159
Email:	suleiman@jlab.org
Date:	April 28, 2016
Department/Division:	Center for Injectors and Sources / Accelerator Division
Other Personnel:	
Proposal Term:	**From:** 10/2015 **Through:** 10/2018 **2nd year** **If continuation, indicate year (2nd/3rd):**

Division Budget Analyst	Tom Wilhelm
Phone:	(757) 269-6426
Email:	wilhelm@jlab.org

Abstract

This LDRD proposal aims to generate and characterize magnetized electron beams from a DC high voltage photogun. Simulations and corresponding measurements of beam magnetization as a function of laser pulse dimension and magnetic field strength at the photocathode are planned. Round-to-flat beam transformation will be performed using three skew quadrupoles and the transverse emittance ratios will be measured. Photocathode lifetime at milli-ampere currents will be compared to beam lifetimes with no magnetization, to study the effect of the solenoid field on photocathode ion-back bombardment. Afterwards, a follow-up proposal can be submitted to evaluate the merits of magnetized beam generation using a DC high voltage thermionic gun, with rf-pulsed gridded thermionic emitter. Combined, these simulations and measurements will benchmark our design tools and provide insights on ways to optimize the JLEIC electron cooler, and help us choose the appropriate electron source and injector layout.

1.0 Summary of Proposal

1.1 Description of Project

To achieve the required luminosity, ion beams at JLEIC must be cooled. In general, this is accomplished when an electron beam co-propagates with an ion beam moving at the same average velocity ($\langle\gamma_e\rangle = \langle\gamma_i\rangle$), but different temperatures ($T_e \ll T_i$), where the energy of chaotic motion of the ion beam is transferred to the cold electron beam. As proposed by Derbenev [1], the cooling rate can be improved by about two orders of magnitude if the process occurs inside a solenoidal field that forces the electrons to follow small helical trajectories thereby increasing the interaction time with ions and improving the cooling efficiency. This cyclotron motion also provides suppression of electron-ion recombination. Cooling rates with magnetized electron beam are ultimately determined by electron longitudinal energy spread rather than the electron beam transverse emittance as the transverse motion of the electrons is quenched by the magnetic field.

The envisioned JLEIC magnetized cooler is part of the Collider ring and aims to counteract emittance degradation induced by intra-beam scattering (IBS), to maintain emittance during collisions and extend the luminosity lifetime. To implement cooling at relatively high energy (electron beam energy 55 MeV (γ=108)), the electron beam must be bunched and accelerated in an SRF linac. The JLEIC cooling solenoid is 30 m long providing a 2 T field. Table 1 summarizes the requirements on the electron beam with noteworthy challenges related to bunch charge and average current, 420 pC and 200 mA, respectively.

Table 1: Requirements on bunched electrom beam for JLEIC magnetized cooling (at the cooling section).

Bunch length (full)	60 ps (2 cm)
Repetition rate	476.3 MHz
Bunch charge	420 pC
Peak current	7.0 A
Average current	200 mA
Beam radius at cathode – flat-top	1.56 mm
Transverse normalized emittance	10s microns
Solenoid field at cathode	2 kG

One challenge associated with implementing cooling inside the long solenoid of the Collider, is the fringe field immediately upstream of the cooling solenoid. The field lines outside the solenoid magnet introduce very large beam rotation. Derbenev [2] suggested the ill-effects of this fringe field could be cancelled if the electron beam was born in a similar field, but producing beam rotation in the opposite direction, such that the two cancel.

Although, electron cooling with DC electron beams at low energy has been implemented at many labs, no one has yet demonstrated electron cooling with bunched electron beams, or magnetized cooling. Fermi Lab successfully demonstrated non-magnetized relativistic DC cooling at high energy (4.3 MeV) [3]. For Low Energy RHIC Electron Cooling (LEReC) non-magnetized bunched electron beam will be used and eRHIC is planning to use Coherent Electron Cooling (CeC) [4,5].

There are four electron gun options to consider: SRF gun, Normal conducting RF gun (with a photocathode or gridded thermionic cathode), DC high voltage gun (with downstream bunching, or rf-pulsed gridded thermionic emitter), and a DC high voltage photogun.

In general, RF guns are more complicated and expensive compared to DC guns. The biggest challenge for a normal conducting RF gun is thermal heat load management. Typically, normal RF guns are used for pulsed-rf applications. Groups have tried to operate normal conducting RF guns in CW mode but so far, with little success (Los Alamos), or with very low resultant beam energy, comparable to (or lower than) energy produced by DC high voltage photoguns (AES, FarTech). The quarter wave VHF gun developed at LBNL as the source for LCLSII is theoretically on the right track, but so far has had difficulty with field emission from the cathode area. Magnetizing this gun would make this problem worse. SRF guns promise CW operation and with high average current and beam energy, but to date, no effort has come close to achieving the desired high average current (Rosendorf, BNL). Moreover, no attempt has been made to produce magnetized beam from an SRF gun, because the application of a magnetic

field on the photocathode is highly problematic to maintaining the superconducting condition of the SRF cavity due to the Meissner effect.

A DC high voltage rf-pulsed gridded thermionic gun, similar to that used at TRIUMF [6], is a viable option since the requirement on gun emittance is not stringent. Of all electron gun options, thermionic guns are considered the closest to “turn-key” technology, relatively simple to operate and maintain, even at very high average current. However, the beam requirements of the Energy Recovery Linac (ERL) may necessitate a smaller emittance from the gun.

Thus we are left with the DC high voltage photogun option. Compared to thermionic guns, photoguns allow for precise control of the electron bunch profile in space and time, which could help to increase the cooling efficiency. Two drawbacks of the dc high voltage photogun are field emission at high bias voltage and the reliance on a relatively delicate photocathode. The JLab gun group has made progress toward minimizing/eliminating field emission. In addition, the gun group has recently manufactured alkali-antimonide photocathodes, shown to be less sensitive to ion bombardment, and demonstrating long lifetime at milli-ampere currents. Based on these considerations, and including our expertise with photoguns, a DC high voltage photogun is the focus of this LDRD proposal.

We also note that a follow-up to this proposal could be submitted to study magnetized beam created using a DC high voltage thermionic gun, with rf-pulsed gridded thermionic emitter. We recently helped TRIUMF develop such a gun, by lending them our original 100 kV thermionic gun. They modified this gun to include the application of rf to the bias grid, and successfully produced rf-bunched beam at high average current and 650 MHz repetition rate, with 100 ps pulses. This gun could be returned to JLab for tests using the same diagnostic beamline and gun solenoid described below.

Examining Table 1, three challenging requirements can be identified. First, the average current is very large. We note that groups from other labs and universities are working hard to achieve high average current and high bunch charge for a variety of applications. The Cornell University group, for example, has recently delivered 65 mA for about 9 hours with lifetime of 2.6 days [7]. Key to this success was the re-discovery of alkali-antimonide photocathode, which is less sensitive to ion bombardment. At JLab, we have used the K_2CsSb photocathode to demonstrate long-lifetime operation at 10 mA average current [8]. The second challenge relates to high bunch charge at high repetition rate. For a DC high voltage gun, this means the gun must be biased at very high voltage, to create a “stiff” beam that is less susceptible to space charge force. We have made relatively good progress developing a 350 kV gun. This work is on-going. The final challenge is the generation and transportation of magnetized bunched electron beam from a gun. Although many labs are pursuing electron cooling, to the best of our knowledge, only one group has been studying *magnetized beam*: the Piot group at the Fermilab Photoinjector Laboratory [9,10]. However, they are not making CW beam at high average current – the new Fermi Lab ASTA injector relies on a pulsed NCRF gun with a Cs_2Te photocathode illuminated by an ultraviolet (UV, λ=263 nm) laser pulse at 0.5% duty factor [11]. No outside groups appear to be working to develop high average current magnetized beam. This is a very serious problem for the JLEIC and the reason we assert the proposed LDRD is essential for JLab.

When discussing magnetized electron cooling, two fundamental topics are involved. The first topic is the interaction between electrons and ions in a longitudinal magnetic field where the presence of a strong field drastically changes the dynamics of the interaction. The second topic is electron beam dynamics in a solenoid magnetic field where the effect of the fringe radial field is accounted for. There are two different motions: one is the helical cyclotron motion in the uniform longitudinal solenoid field due to the transverse velocities of the electrons arising from finite emittance. This motion has a very small radius and a very small resultant emittance. The second rotational motion is due to the azimuthal kick from the fringe radial field at the entrance or exit of a solenoid. This motion has a very large radius (the radius is half of the initial radial displacement of the electron from the solenoid axis) and a very large resultant emittance. For a focusing solenoid, the beam enters and exits the solenoid and the two azimuthal kicks cancel each other. For magnetized electron cooling, the electron beam is being used inside the cooling solenoid (where it suffers an azimuthal kick when it enters). This kick is cancelled by an earlier kick at the exit of the cathode solenoid where the electron beam was born inside it.

The narrative of magnetized electron cooling is described below using cylindrical coordinates (r,ϕ,z) with the vector momentum written as: $\vec{\boldsymbol{p}} = p_r\hat{\boldsymbol{r}} + p_\phi\hat{\boldsymbol{\phi}} + p_z\hat{\boldsymbol{z}}$. (Boltzmann constant, k_B = 8.617x10^{-5} eV/K, m_ec^2 = 510998 eV, c = 299792458 m/s, e/m_e = 1.759x10^{11} rad/(s T)):

1. Electrons are born in a uniform magnetic field $B_{cath} = B_z$ = 0.2 T where the electron beam Gaussian sigma is a_0 = 3 mm (this is the same as the laser spot size). The K_2CsSb photocathode effective temperature is about T_{eff} = 1000 K (with 532 nm green laser). For this cathode the transverse thermal energy is k_BT_{eff} = 0.086 eV, the transverse momentum is $p_{\perp 0} = \sqrt{2m_ek_BT_{eff}}$ = 296.8 eV/c and the thermal emittance is $\epsilon_{th} = a_0\frac{p_{\perp 0}}{2m_ec} = a_0\sqrt{\frac{k_BT_{eff}}{2m_ec^2}}$ = 0.87 μm.
2. For a gun HV of 350 kV, β = 0.8048, γ = 1.685 and the momentum in the z direction is p_z = βcγm$_e$ = 693 keV/c.
3. Since the electrons are born with transverse thermal momentum in magnetic field, each electron will have a helical cyclotron motion with radius $r_c = \frac{p_{\perp 0}}{eB}$ = 4.95 μm. This cyclotron radius is very small when compared to the electron beam radius. The cyclotron frequency is $\omega_c = \frac{eB_z}{\gamma m_e}$ = 2.09x10^9 rad/s.
4. The emittance (cyclotron emittance) due to cyclotron motion is: $\epsilon_c = \frac{k_BT_{eff}}{eB_zc}$ = 0.00144 μm; very small when compared to thermal emittance.
5. After traveling a few centimeters from the photocathode, the electrons exit the longitudinal solenoid field but they encounter a returning solenoid radial field which exerts torque on the electrons that produces a rotating trajectory. This beam rotation must be tailored to cancel out similar motion encountered when entering the field of the cooling solenoid.

6. Busch's theorem represents the conservation of canonical angular momentum (CAM) and states that $L = \gamma m_e r^2 \dot{\phi} + \frac{e}{2\pi}\psi$ is a constant, where $\dot{\phi} \equiv \frac{d\phi}{dt}$ is the angular velocity and $\psi = \int \boldsymbol{B} \cdot d\boldsymbol{S}$ is the magnetic flux enclosed by the particle trajectory (i.e., the flux inside a circle with radius *r* given by the radial distance *r* of the particle from the z-axis).
7. From Busch's theorem, at the photocathode, $L = \frac{e}{2\pi}\psi$ and $\psi = \int \boldsymbol{B} \cdot d\boldsymbol{S} = \pi r^2 B_z$, that is for an electron $L = \frac{1}{2} e B_z r^2$. And after leaving the solenoid $L = \gamma m_e r^2 \dot{\phi}$.
8. For cylindrically symmetric gaussian beam with sigma of a_0, $\langle r^2 \rangle = 2a_0^2$ and the average canonical angular momentum for the electron beam is $\langle L \rangle = e B_z a_0^2$ = 1800 (neV s) at the photocathode and $\langle L \rangle = 2\gamma m_e a_0^2 \dot{\phi}$ = 1800 (neV s) after existing the solenoid. Note: For cylindrically symmetric flat-top beam with radius a_0 = 1.56 mm, $\langle r^2 \rangle = \frac{a_0^2}{2}$ and the average canonical angular momentum for the electron beam is $\langle L \rangle = \frac{e B_z a_0^2}{4}$ = 122 (neV s) at the photocathode and $\langle L \rangle = \frac{\gamma m_e a_0^2 \dot{\phi}}{2}$ = 122 (neV s) after existing the solenoid.
9. For cylindrically symmetric gaussian beam with sigma of a_0, $\langle r \rangle = \sqrt{\frac{\pi}{2}} a_0$ and for cylindrically symmetric flat-top beam with radius a_0, $\langle r \rangle = \frac{2}{3} a_0$.
10. The average angular velocity is $\dot{\phi} = \omega_L = \frac{e B_z}{2\gamma m_e}$ = 1.04x10^{10} rad/s (i.e., the beam rotates at the Larmor frequency, $\omega_L = \frac{\omega_c}{2}$). The average mechanical momentum in the ϕ direction is $p_\phi = \sqrt{\frac{\pi}{2}} \gamma m_e a_o \dot{\phi}$ = 112.72 keV/c. The electron momentum now has a phi component in addition to the axial z-component.
11. The average rotational kinetic energy is $T_\phi = \sqrt{(m_e c^2)^2 + p_\phi^2 c^2} - m_e c^2$= 12284.7 eV. This is small (only 3.51%) when compared to the maximum longitudinal kinetic energy of T_z = 350000 eV. The total kinetic energy is still $T_z + T_\phi = 350000$ eV (i.e., part of the longitudinal (axial) kinetic energy turns into rotational energy in the phi direction).
12. The electron beam leaves the cathode solenoid field rotating and acquires an angular momentum but once in field-free region where there is no centripetal force, the beam rotates and simultaneously expands as it propagates. As it expands, its angular velocity decreases to conserve angular momentum.
13. The beam size increases as the beam propagates such that the angular momentum of the beam is conserved. Focusing solenoids installed after the exit of the gun and throughout the injector prevent the magnetized beam from blowing up.
14. After leaving the cathode solenoid, and due to beam rotation induced by radial field the *magnetized beam* will have an emittance (called drift or magnetized

emittance) of $\epsilon_d = \frac{eB_z a_0^2}{2m_e c}$ = 528 μm, or in general, ϵ_d[μm] ~ 29.3 B [kG] σ_e^2 [mm]^2. Note: For flat-top beam with radius a_0 = 1.56 mm, the drift or magnetized emittance is $\epsilon_d = \frac{eB_z a_0^2}{8m_e c}$ = 36 μm, or in general, ϵ_d[μm] ~ 7.3 B [kG] r_e^2 [mm]^2.

15. The cyclotron emittance and drift emittance are related as $\epsilon_{th} = \sqrt{\epsilon_c \epsilon_d}$ where the ratio is $\frac{\epsilon_d}{\epsilon_{th}} = \sqrt{\frac{\epsilon_d}{\epsilon_c}} = \frac{a_0}{r_c}$ = 606.
16. The electron beam is accelerated in SRF linac to high energy.
17. The magnetized beam is a coupled beam, and for the kicker section in the circulator-cooler ring, it is easier if the beam is transformed to a flat beam. This can be done with three skew quads (aka, Round-to-Flat Beam (RTFB) Transformer). This transformation produces a beam with very large transverse emittance ratios. For round beam, $\epsilon_x = \epsilon_y$, in contrast to flat beam where $\epsilon_x \gg \epsilon_y$.
18. Bush's theorem states that CAM is preserved in any axisymmetric magnetic field. A quadrupole triplet does not do so; ultimately it can turn CAM to zero (in case when the cyclotron emittance is zero, i.e., practically very small compared with the drift one) and also restore it later when needed.
19. If the beam was transformed to flat in the kicker section, then before entering the cooling solenoid, the beam is transformed back to round beam (magnetized beam) with Flat-to-Round Beam (FTRB) Transformer that restores the initial magnetization.
20. At the entrance of the cooling solenoid, the radial field exerts a torque (opposite to cathode solenoid torque) so the beam is not rotating any more (note that the magnetic field in both solenoids must be in the same direction). This can be achieved when $B_{Cath} a_0^2 = B_{cool} \sigma_e^2$, where B_{cool} = 2.0 T and electron beam radius in the cooling section is σ_e = 0.95 mm.
21. Typical radius of the ion beam in the cooling solenoid is 1.0 mm with normalized emittance of about ϵ_{ion}^n = 0.4 μm. The cooling in the Collider ring aims to maintain this low emittance. The effect of the fringe radial field on ions is suppressed by the ratio of the ion mass to the electron mass (m_p/m_e = 1836).
22. Once inside the cooling solenoid, the electrons only have a cyclotron motion with radius $r_c = \frac{p_{\perp 0}}{eB}$ = 0.49 μm but no rotational motion due to the fringe radial field. The cyclotron emittance due to this motion is $\epsilon_c = \frac{k_B T_{eff}}{eB_{cool} c}$ = 0.000144 μm.
23. If the beam is not magnetized from the gun, then the additional rotational motion when it enters the cooling solenoid will make it much hotter than the ion beam (ϵ_d = 528 μm). Instead the emittance will be very close the thermal emittance from the cathode – since the cyclotron emittance is very small (albeit with some degradation due to space charge emittance growth but this can be compensated with focusing solenoids in the beamline).

24. Hence: if the beam is not magnetized from the gun then no cooling can take place in a solenoid. Furthermore, magnetic shielding is now needed in the cooling section; non-magnetized cooling has very strong dependence on relative angles between electrons and ions and strict control of remnant magnetic fields is required to minimize the transverse angular spread in the cooling section.
25. In the cooling solenoid, the electron energy is 55 MeV, with β = 0.999957 and γ = 107.63.
26. For magnetized beam in the cooling solenoid, the cyclotron frequency is $\omega_c = \frac{eB_{cool}}{\gamma m_e}$ = 3.27x10^9 rad/s, or $f_c = \frac{\omega_c}{2\pi}$ = 0.52 GHz. Over the length of the cooling solenoid of 30 m, the electron will finish $n = \frac{L}{\beta c} f_c$ = 52 periods of its cyclotron rotations.
27. The helical motion of the electrons in the magnetic field increases the electron-ion interaction length, thereby significantly improving the cooling efficiency. In particular, electron-ion collisions that occur over many cyclotron oscillations and at distances larger than the cyclotron radius are insensitive to the transverse velocity of the electrons. This cyclotron motion also provides suppression of electron-ion recombination.
28. In general, electron cooling is preferred at low energy. At higher energies the cooling rate picks up a factor of $1/\gamma^2$ due to Lorentz contraction and time dilation. In the electron-ion rest frame, the length of the cooling solenoid is only 30/γ = 0.28 m. In addition, in their rest frame, the electron and ion stay together for only 30/(βcγ) = 90/γ = 0.84 ns.
29. Electron-ion collisions are described by Rutherford's scattering formula and is determined (and hence the cooling rate) by the relative particle velocities' spread, $\Delta(\overrightarrow{v_e} - \overrightarrow{v_i})$ in the co-moving frame ($\overrightarrow{v_\perp} = \gamma c\vec{\theta}$, $\overrightarrow{v_\parallel} = c\Delta\gamma/\gamma$), where $\vec{\theta}$ is the transverse angle deviations.
30. For non-magnetized beam, the cooling rate is $\lambda \propto 1/v_{e\perp}^3$ while for magnetized beam, the cooling rare is $\lambda \propto 1/(v - v_{e\parallel})^2$. Electron beam energy spread in JLEIC cooler is required to be $\Delta\gamma_e/\gamma_e \leq 10^{-4}$.
31. Cooling solenoid must have high parallelism of magnetic field lines, $\frac{\Delta B_\perp}{B} \approx \sqrt{\frac{\epsilon_{ion}^n}{\beta\gamma\beta_{match}}} \approx 10^{-4}$, where ϵ_{ion}^n = 0.4 μm is the ions normalized emittance and β_{match} = 0.18 m is the beta function in the cooling solenoid.
32. Upon exiting the cooling solenoid, the beam once again starts rotating due to canonical angular momentum conservation according to Busch's theorem.
33. The spent electron beam enters the Energy Recovery Linac (ERL) and then dumped at low energy.

Figure 1 shows a depiction of the magnetized electron cooling process.

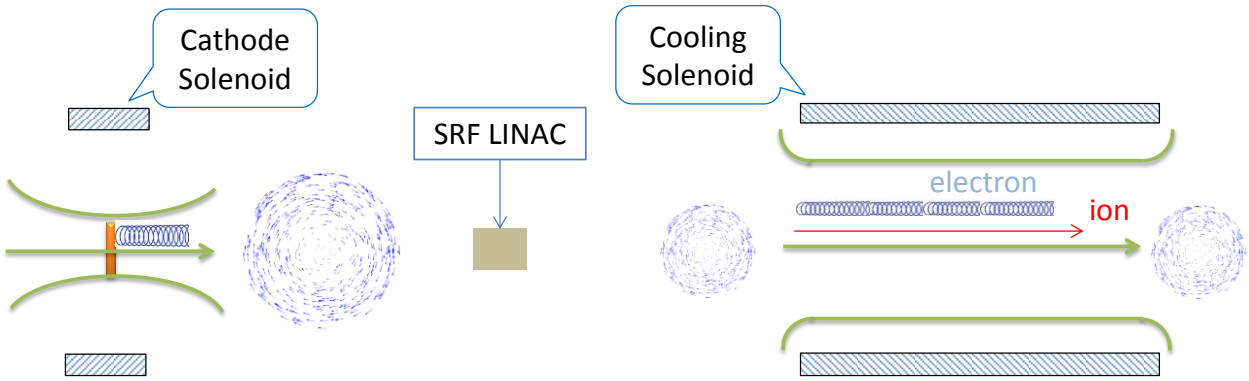

Figure 1: Depiction of magnetized electron beam generation and magnetized cooling in a solenoid.

1.2 Expected Results

This LDRD will generate and characterize magnetized electron beams from a DC high voltage photogun. Expected results include:

- JLab will have direct experience magnetizing a high current electron beam.
- We will learn how the applied magnetic field influences the photocathode lifetime.
- We learn about challenges associated with Round-to-Flat Beam (RTFB) transformations at high bunch charge.
- We will benchmark our simulation tools in this new space-charge dominated, magnetized regime.

2.0 Proposal Narrative

2.1 Purpose/Goals

The goal of this LDRD is to generate a magnetized beam and measure its properties. The simulations and corresponding measurements will provide insights on ways to optimize the JLEIC electron cooler, and help us design the appropriate electron source. Below we will describe the proposed measurements and simulation plans.

2.2 Approach/Methods

Experimental Overview:

A schematic layout of the experimental beamline is shown in Figure 2. We will use the gun and injector beamline that is being built now at the Gun Test Stand (GTS) to carry out the proposed LDRD work. Some modification to the beamline will be required, noticeably the installment of skew quadrupoles for the RTFB transform. We will follow

the prescription outlined in Ref. [12] to design the three skew quadrupoles. Simulations will be used to determine the appropriate location of the diagnostic crosses.

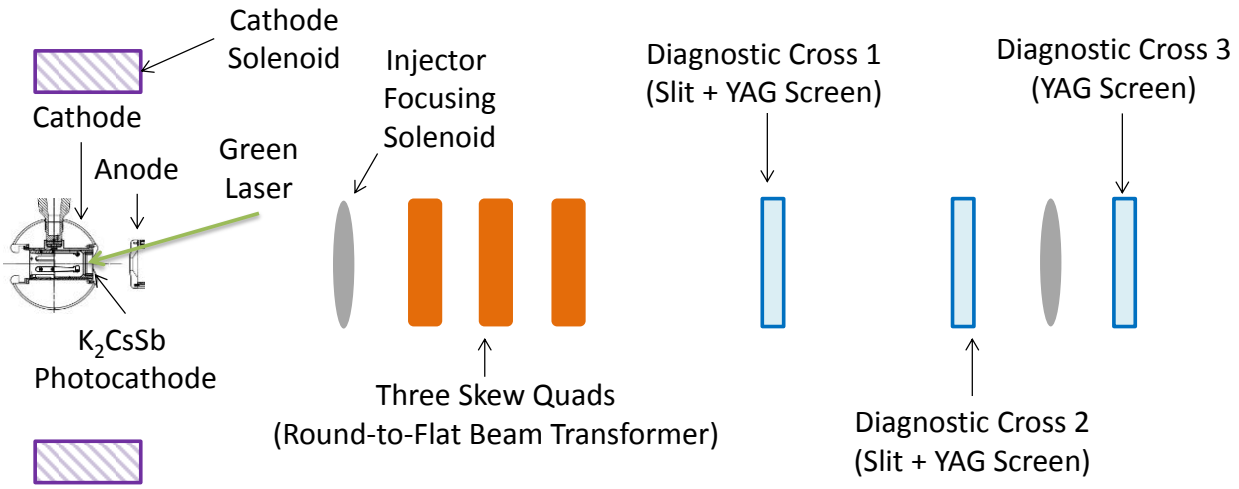

Figure 2: Proposed beamline to generate magnetized beam and measure beam magnetization. Focusing solenoids will be installed between the gun and dump to prevent the magnetized beam from blowing up.

The gun is an inverted ceramic with a K_2CsSb photocathode and a green 532 nm drive laser (with repetition rates of 15 Hz to 476.3 MHz). We have two HV supplies: Spellman 225 kV and 32 mA and Glassman 550 kV and 5 mA (with SF_6 system). Figure 3 shows the HV chamber. For the proposed LDRD work we need to design and build a solenoid to produce 2 kG at the photocathode with uniformity over the active area to be specified as part of this project.

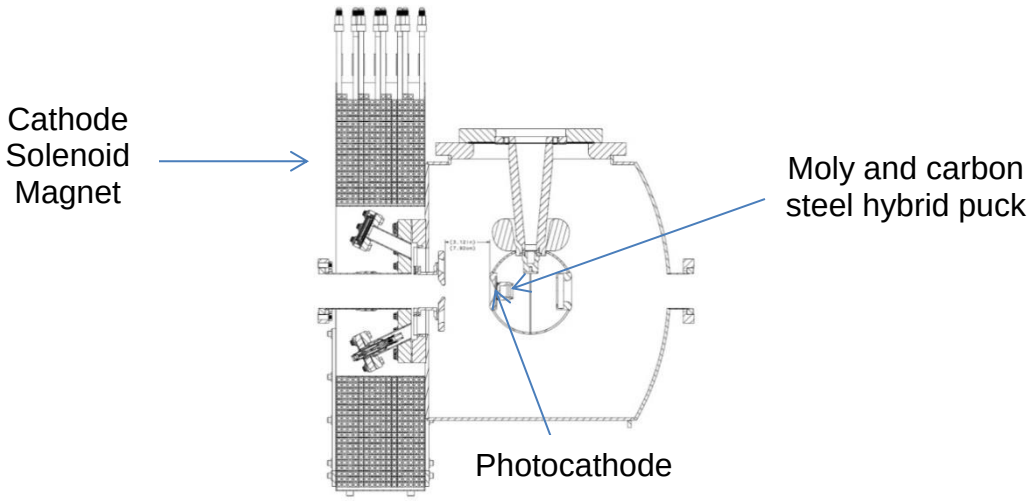

Figure 3: HV chamber with inverted ceramic and a ball cathode. A solenoid magnet will be installed in front of the chamber to generate uniform field at photocathode.

Simulation Plan:

The electron beam parameters from the injector required to meet the JLEIC cooling specification are unique. Producing low energy, magnetized beam that is space charge dominated has not been previously investigated in depth by the accelerator community. We will use simulation tools to create a physics design for the beamline so we can locate magnets and diagnostics at their optimum positions. Simulation of different operating scenarios of bunch charge, magnetization, bunch shape etc. will be benchmarked against measurements of emittance and other beam parameters (detailed below). As the beams will be space charge dominated, there will be some limit to the aspect ratio that can be achieved with the RTFB transform. Simulation will allow us to quantify how good or complete this can be made for different settings. These results will guide the design of the JLEIC injector in the future.

To speed up the benchmarking process, we would ideally like to automate the process of measurement taking and comparison to a virtual machine. This can be achieved using a free Matlab to EPICS interface (as used at SLAC and Cornell University). Matlab scripts can then be used to take measurements and simulate those conditions for comparison, using actual component settings as input.

Measurement Plan:

1. Generate magnetized beam and measure magnetization for different laser spot sizes, (a_0 = 1 – 5 mm), bunch charges (1 – 500 pC), bunch lengths (10 – 100 ps) and solenoid fields (0 – 2 kG). The magnetization will be measured using Diagnostics Cross 1 and Diagnostic Cross 2 with the three skew quads off via

$$\langle L \rangle = 2p_z \frac{\sigma_1 \sigma_2 \sin\phi}{D} = eB_z a_0^2$$

where σ_1 is the beam radius measured at Diagnostic Cross 1 and σ_2 is the beam radius measured at Cross 2. The drift between the two crosses is D and p_z is the longitudinal momentum of the beam (for a gun HV of 350 kV, $p_z = \beta\gamma m_e$ = 693 keV/c). The angular rotation ϕ (see Figure 4) is measured from the beam image at Diagnostics Cross 2 when the slit is inserted at Diagnostics Cross 1. Figure 5 shows an example of a mechanical measurement done at Fermilab.

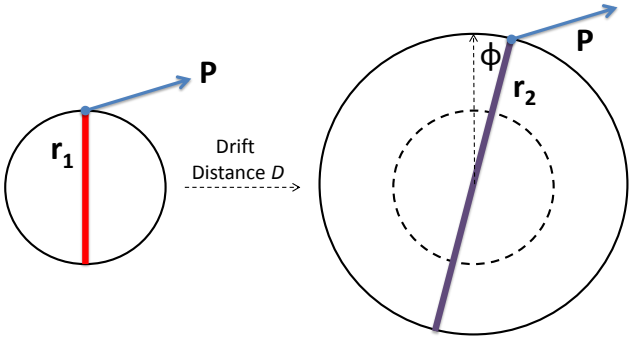

Figure 4: Simultaneous expansion and rotation of a beam with angular momentum in a field-free region.

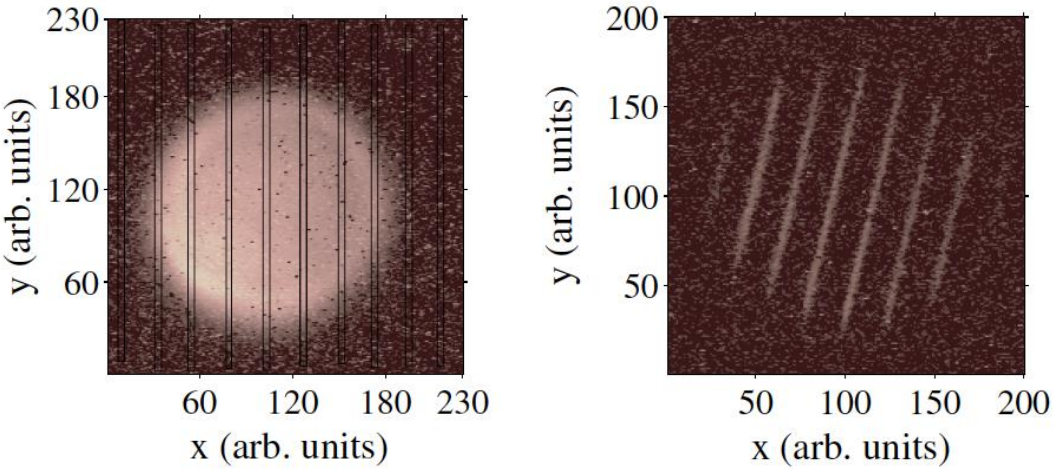

Figure 5: Example of data set used for mechanical angular momentum measurement at Fermilab. Figure from Ref. [9].

2. Use the three skew quads – RTFB Transformer proposed by Derbenev [13] – to generate a flat beam with transverse emittance ratios of $\frac{\epsilon_x^n}{\epsilon_y^n} = \frac{\epsilon_d}{\epsilon_c} = \frac{r_c^2}{a_o^2} \gg 1$.

   The horizontal and vertical emittance will be measured using the slit method. Diagnostics Cross 2 will be equipped with a horizontal and vertical slits. The size of the emittance dominated beamlets passed through the slits will be measured, after a drift distance *D*, with a YAG viewer in Diagnostics Cross 3. Assume that the horizontal beam radius measured at Diagnostics Cross 2 is σ_{2h} and the horizontal radius of the beamlet at Diagnostics Cross 3 is σ_{3h} when a vertical slit is inserted at Diagnostics Cross 2, then the horizontal emittance is $\epsilon_x^n = \gamma\sigma_{2h}\sigma_{3h}/D$. Similarly the vertical emittance can be measured using a horizontal slit.

3. Generate very high currents magnetized beam and study beam transport and RTFB transformation versus electron bunch charge.
4. Measure magnetized photocathode lifetime at high currents (up to 32 mA) and high voltages (200 – 350 kV).
5. Study beam halo and beam loss versus magnetization. We can do that using three different techniques:
   I. Use ion pumps equipped with very sensitive current readback to monitor vacuum.
   II. Radiation will also be monitored using x-ray detectors placed around the gun and beamline.
   III. We will measure the beam intercepted at the floating anode.

2.3 Specific Location of Work

The work will be performed in the LERF Gun Test Stand (GTS). Figure 6 shows the existing beamline that was built as part of FEL program but never used. This beamline will be modified to install the three skew quadrupoles and a beam dump.

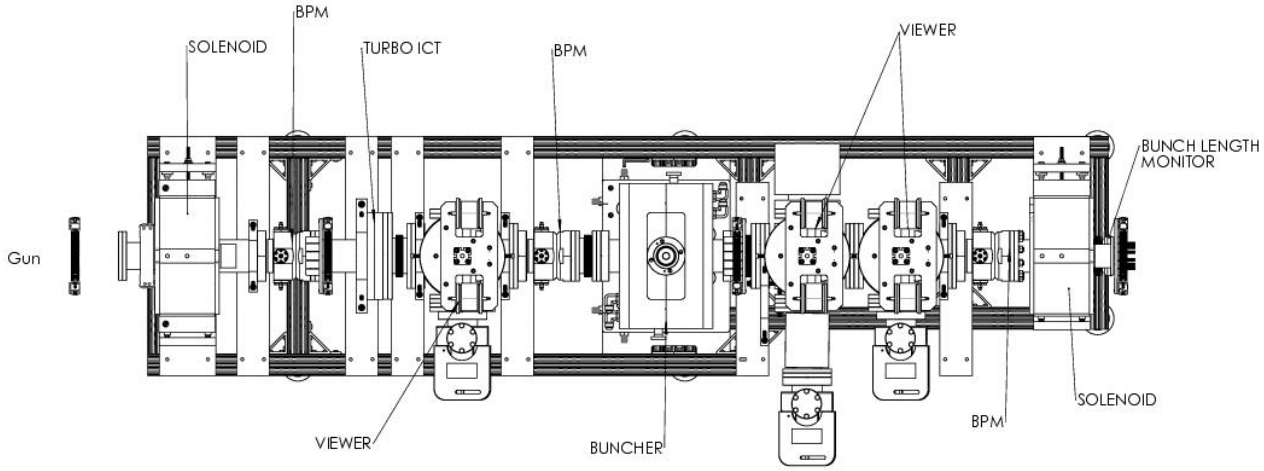

Figure 6: The existing beamline top view. There is no buncher installed; only a drift beamline, where the three skew quads will be installed.

2.4 Anticipated Outcomes/Results

We hope to demonstrate experimentally many aspects of the magnetized bunched electron beam for the JLEIC cooler, with the notable exception of 200 mA average beam current. We are limited by the in-house HV supplies to 32 mA.

- Demonstrate 32 mA magnetized beam at 200 kV
- Quantify any difference in lifetime of K_2CsSb between magnetized and non-magnetized beam
- Measure magnetization for a variety of charge, bunch dimensions, solenoid strength etc. guided by JLEIC specifications.
- Quantify the quality of RTFB transform for a variety of charge, bunch dimensions, solenoid strength etc.
- Demonstrate reliable simulation tools and methods.
- Improve experimental techniques with new machine operation interface.

3.0 Prior Year Accomplishments

3.1 Gun, Preparation Chamber and Beamline

We started with an empty room at the GTS and built a photogun, an alkali-antimonide photocathode preparation chamber and a diagnostic beamline. Figure 7 shows the preparation chamber, gun and beamline in the GTS, all connected, baked and under vacuum. The gun was HV conditioned and is now ready to make beam at 325 kV. The K_2CsSb preparation chamber has been assembled and we successfully grew our first photocathode at GTS on April 25, 2016. The beamline has been instrumented with steering coils, ion pumps and viewers. The GTS OSP is approved for only 10 nA; we are working with Radiation Control Group for approval at full current. We believe RadCon will approve operation at the desired high current via judicious placement of local shielding along the beamline and beam dump. We plan to start making non-magnetized beam at the GTS by early May 2016.

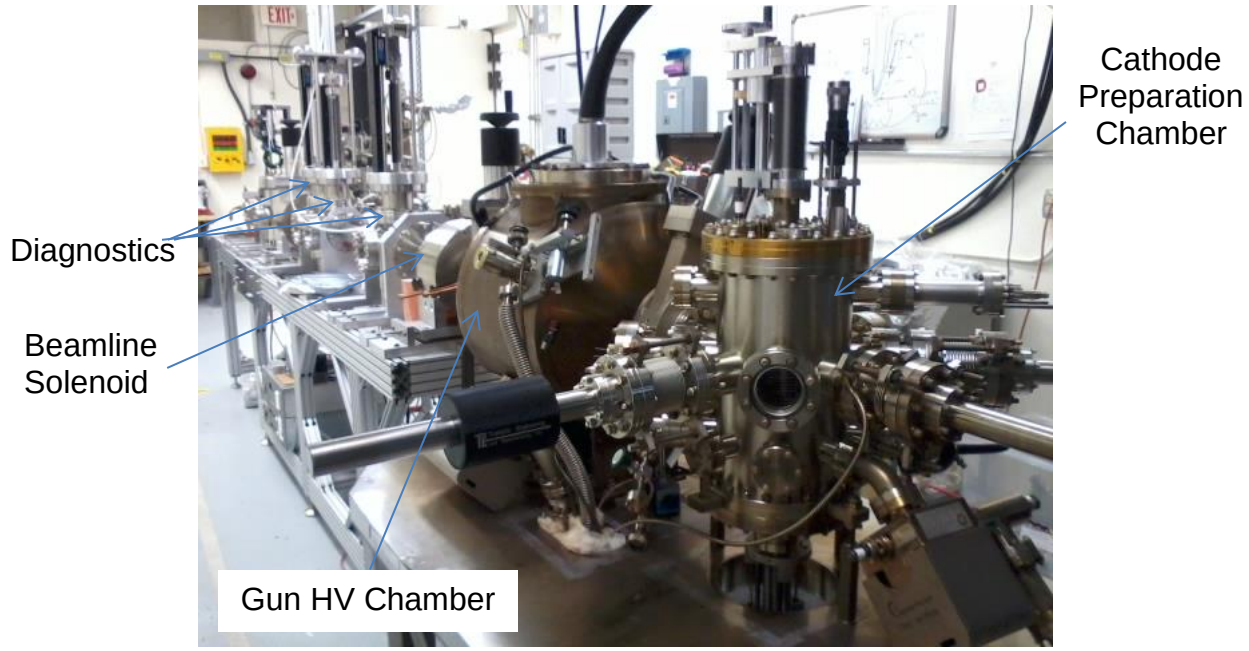

Figure 7: Preparation chamber, gun and beamline in the GTS.

The lasers are ready and the LOSP has been approved. We will have three types of lasers:

1. Amplified Nd:YLF laser system: 15 Hz, 45 ps, green, 1 mJ/pulse energy, 10 mW (average),
2. Verdi laser: DC, green, 10 W and
3. Antares Mode-locked Nd:YLF laser: 74.85 MHz, 60 ps, green, 5 W. To be replaced later with fiber laser at 476.3 MHz.

3.2 Cathode Solenoid Magnet

The cathode solenoid magnet was designed to fit in the front of the gun chamber. Table 2 lists the physical properties of the magnet. The field at the cathode is 1.4 kG when using the standard molybdenum puck. The magnet will be powered by the new CEBAF spare dogleg supply (500A, 80V). The magnet has been procured and is expected to be on site by July 8, 2016.

Table 2: Physical properties of the cathode magnet solenoid. The magnet will be operated at 400 A to provide 1.4 kG at cathode.

Size	11.811” ID, 27.559” OD, 6.242” Z
Conductor	L=500 m, A=0.53 cm2 (16 layers by 20 turns)
Coil Weight	240 kg
Resistance	0.18 Ω (65°C average T)
Field at photocathode	1.4 kG
Voltage	72 V
Current	400 A

The magnet coil is shown in Figure 8. There are 16 layers along the beam and 20 radial turns. LCW will be used to cool the magnet. The LCW pressure at GTS is 150 psi and the operating temperature is 90˚F.

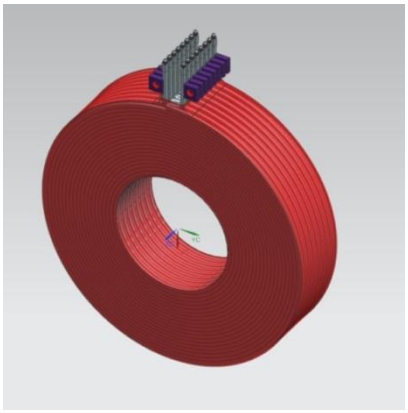

Figure 8: Cathode solenoid magnet. The magnet is made up of 8 double pancakes.

A molybdenum and carbon steel hybrid puck is designed to enhance field at cathode to 2.0 kG. We plan to make 4 pucks and map with solenoid. These 4 pucks will be subjected to the following heat treatment plan – 4 choices:

1. Un-heated,
2. 200˚C (experienced during Sb growth) and 120˚C (experienced during K – Cs growth),
3. 550˚C (experienced during heat cleaning) then 200˚C and 120˚C and
4. Multiple heat cycles.

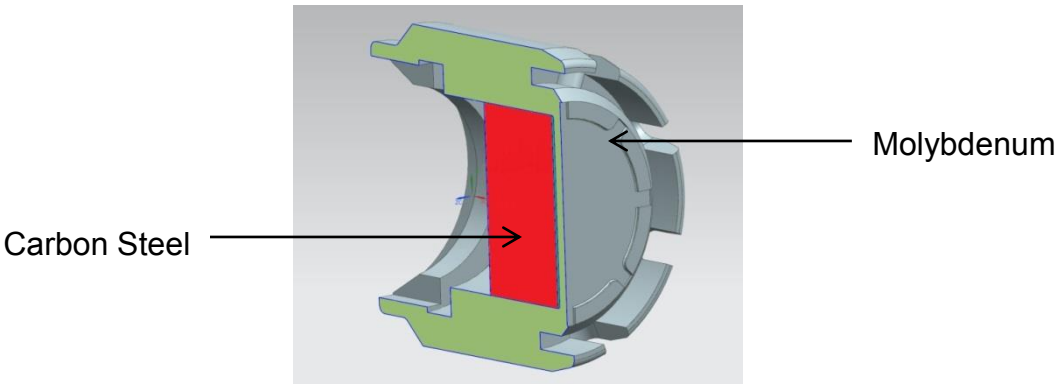

Figure 9: Molybdenum and carbon steel hybrid puck.

Figure 9 shows the new puck design. We will use 1006 carbon steel brazed inside the molybdenum puck. The enhancement of the magnetic field is proportional to the thickness of carbon steel [14]. Because of the current design of pucks, cathode and preparation chamber, the maximum carbon steel that can be added to the puck is limited to about 10 mm. We may opt to make the whole new puck of carbon steel. We plan to map the magnet alone and with the hybrid puck in the Magnet Measurement Facility before installing the magnet in the GTS in August. The plan is to generate magnetized beam by October 1st, 2016.

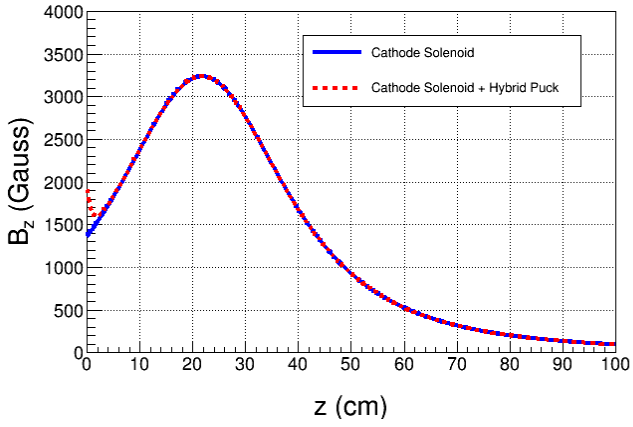

Figure 10: Magnetic fields generated by the cathode solenoid and the carbon steel hybrid puck. The photocathode is at z=0 cm.

The magnetic field, B(0,0,z), as a function of z along the beam path is shown in Figure 10. The magnet will be a bare coil with no steel shielding around it. We will mark the 5 G region around the magnet and develop procedure for safe operation. In particular, we will add interlocks to the GTS concrete shield door and a beacon, to ensure solenoid can only be energized when door is closed.

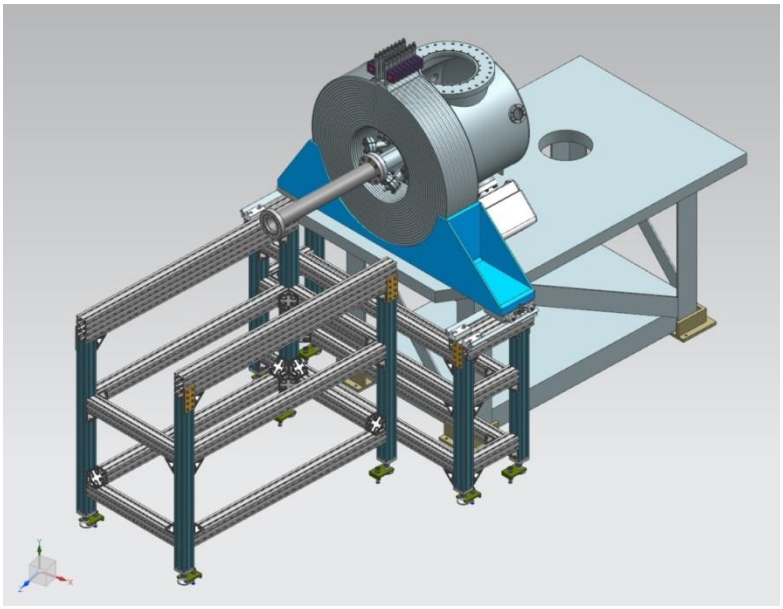

Figure 11: Cathode magnet support structure to be able to push the magnet away from the gun to have space to build an oven to bake the gun chamber to 250˚C.

The magnet will not be bakable. To be able to bake the gun HV chamber, the magnet will be mounted on rails and will be moved downstream away from the gun as illustrated in Figure 11. This will provide enough space to build an oven around the gun. In addition, the magnet support will allow for small adjustments of about 5 mm in both *x* and *y* to center the solenoid on the electron beam.

3.3 Simulations (Fay Hannon)

Simulations of the magnetized beam have been used to determine the beamline layout, the design of the emittance and magnetization measurement diagnostics and the concept of a round to flat transformer.

3.3.1. Magnetized beams

Simulations have shown that a magnetized beam with the properties described in Table 3, are dominated by the transverse canonical angular momentum imparted when exiting the cathode solenoid.

Table 3: Input parameters used in simulation of magnetized beam from a photogun.

Cathode B_z	0.2 T
Radius, flat-top	3.0 mm
t_rms, Gaussian	23 ps
Bunch charge	1 – 420 pC
Gun high voltage	350 kV

Figure 12 shows that irrespective of bunch charge, the transverse beam evolution is practically the same. We hope to confirm this with measurements in FY17. Note that the beam size is large compared to other beams we use at Jefferson Lab. For this reason care will be taken to place transport magnets such that we don't lose any part of the beam on the beam tubes.

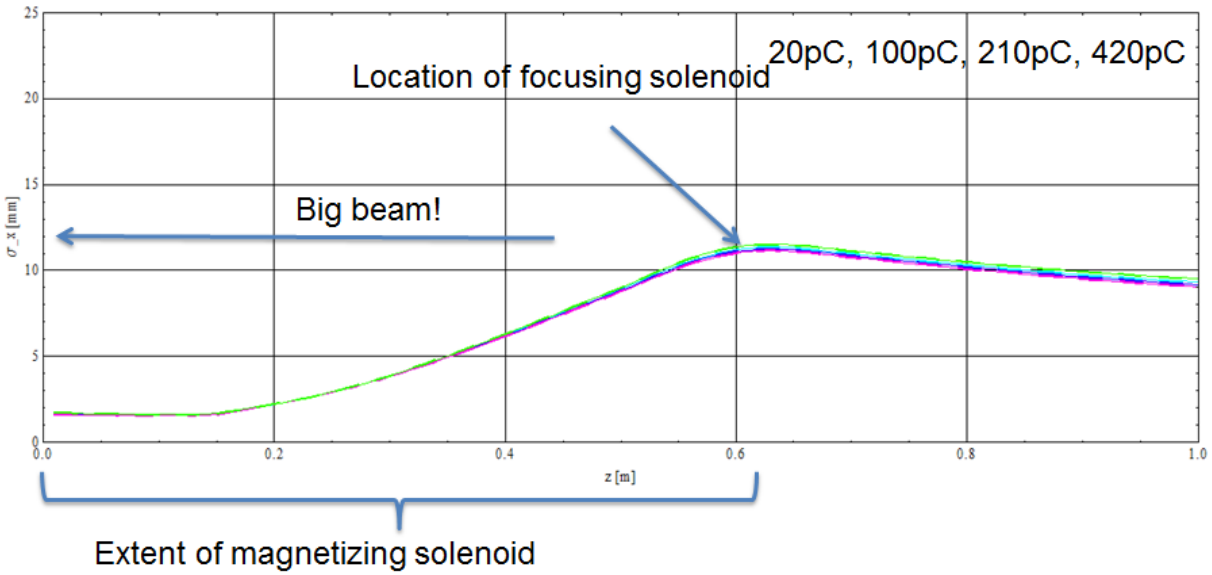

Figure 12: Transverse rms beam size as a function of distance from the cathode. The first diagnostic cross will be placed at 1 m.

Longitudinally, the bunch length propagates as normal, proportional with space charge effects, shown in Figure 13.

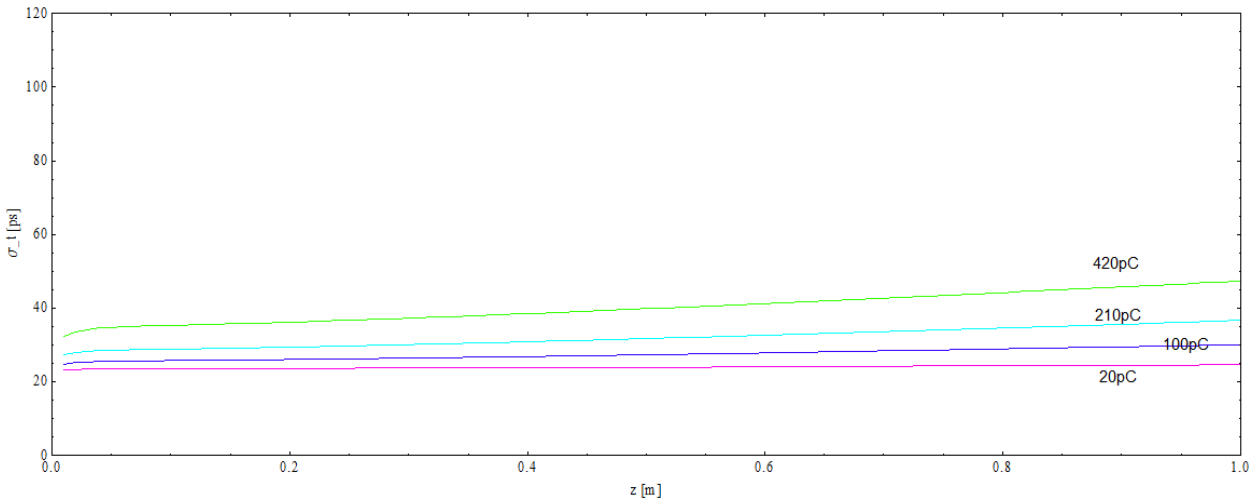

Figure 13: Longitudinal rms bunch length as a function of distance from the cathode. Note we have no mechanism for measuring bunch length with this apparatus.

A number of magnetizing magnet schemes were evaluated for use in the LDRD experiment as shown in Figure 14.

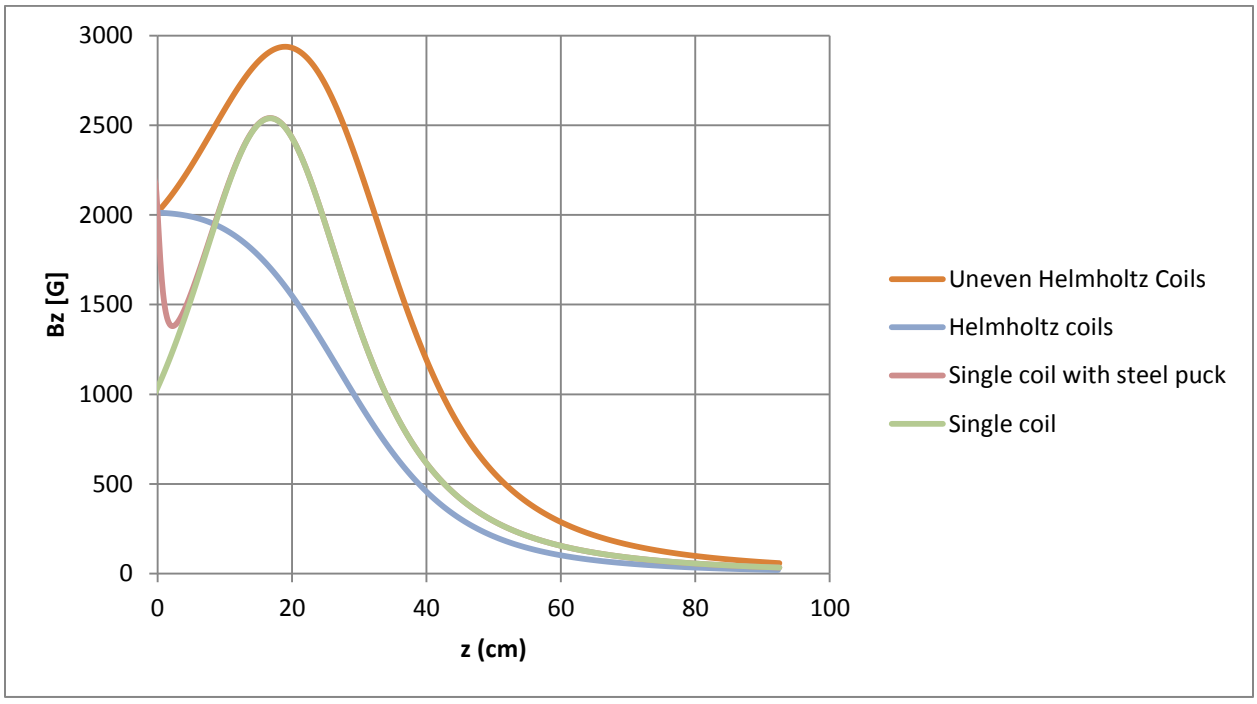

Figure 14: Magnetizing magnet options.

Simulation results from a virtual magnetization measurement experiment (as detailed in the former narrative) show that we can produce a linearly magnetized beam with any of the options, green points in Figure 15. For this reason the most cost effective choice of a single solenoid placed just downstream of the gun flange with the option of a steel puck was chosen for the LDRD experiments.

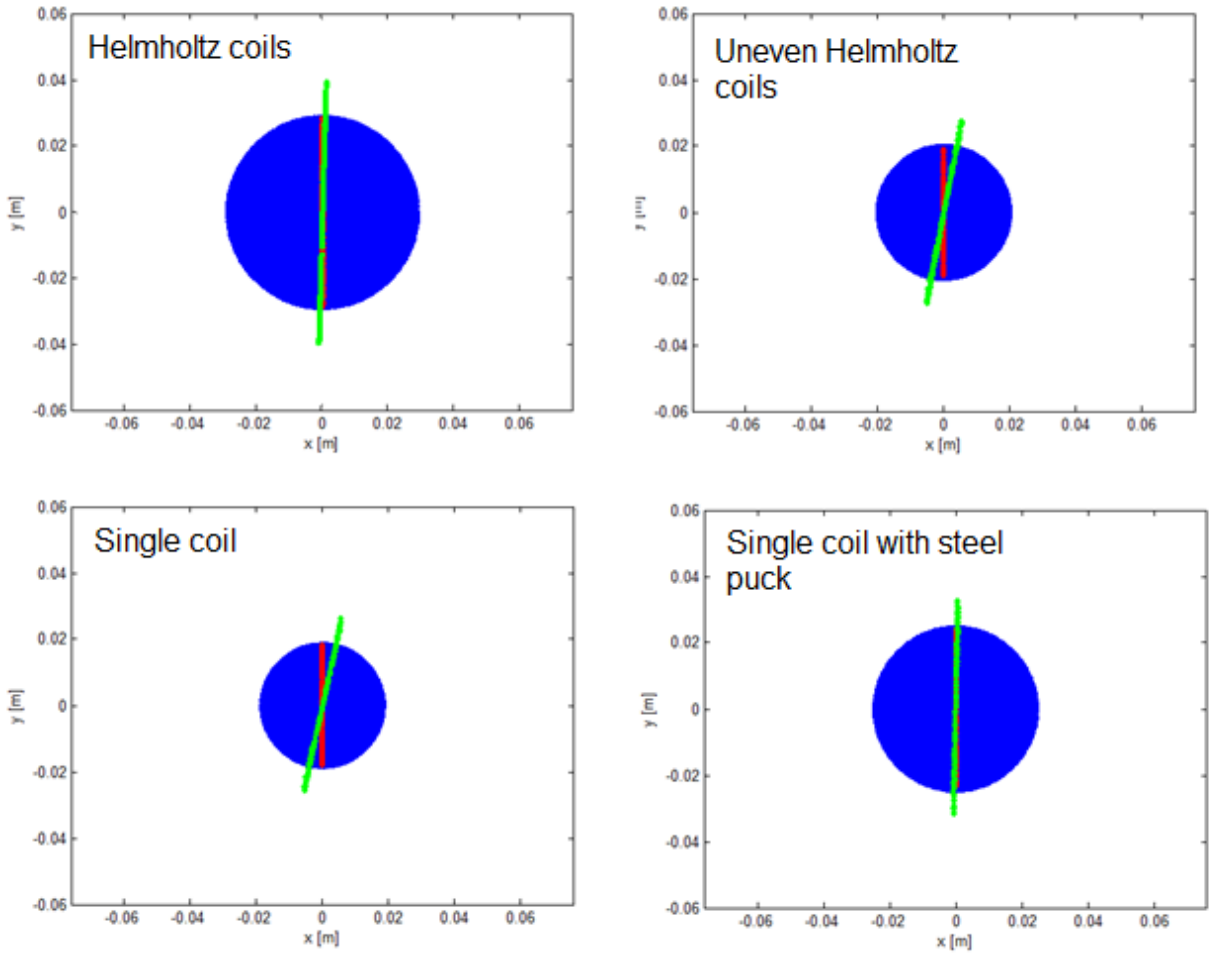

Figure 15: Virtual magnetization measurement simulation. Blue: transverse particle positions at the first diagnostic screen. Red: the particles selected by a 40 μm vertical slit at the first diagnostic. Green: The particle position at the second diagnostic screen.

It will be important to measure the range of electron beam parameters at the cathode. We will vary both cathode radius and field strength, such that the magnetized emittance value remains constant, Figure 16. By measuring lifetime as a function of these settings we can guide the JLEIC cooler design.

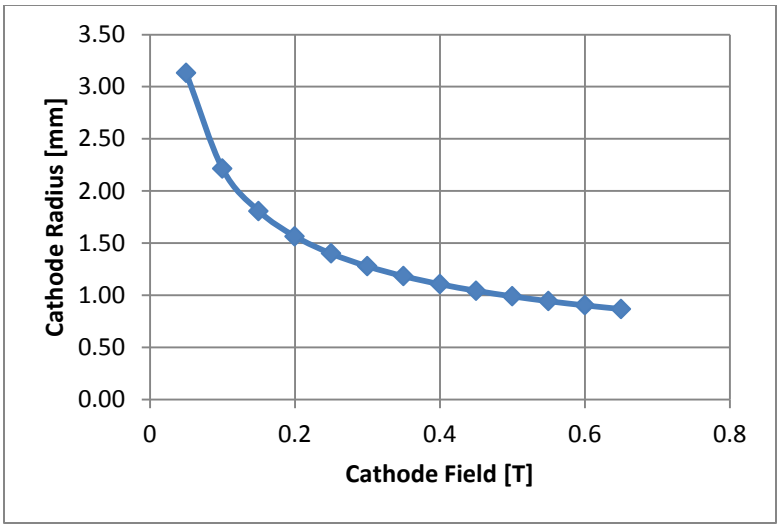

Figure 16: Curve of constant magnetized emittance.

3.3.2. Emittance measurements

We have simulated a virtual experiment to determine the best dimensions of the emittance measurement slit. The double slit measurement technique will be used (shown in figure 17), whereby the electron beam is swept across one slit using a pair of corrector magnets, and then the resulting beamlets are swept across a second slit. A Faraday cup with picoammeter is used to measure charge.

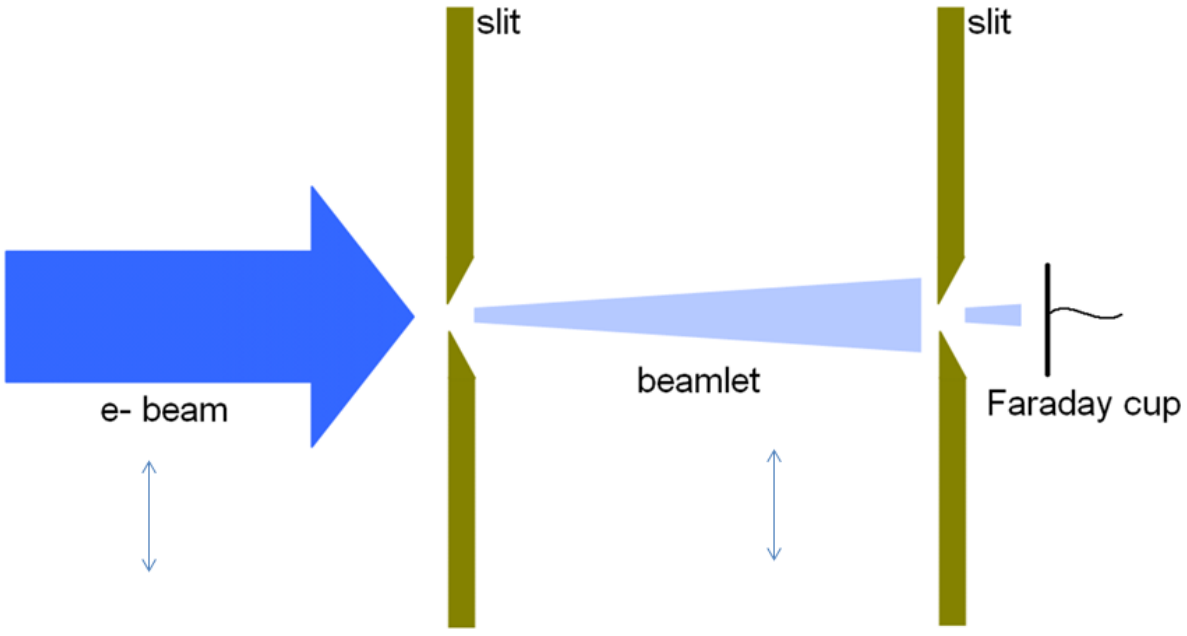

Figure 17: Schematic concept of the double slit emittance measurement technique. The first slit gives position information, the second angular information.

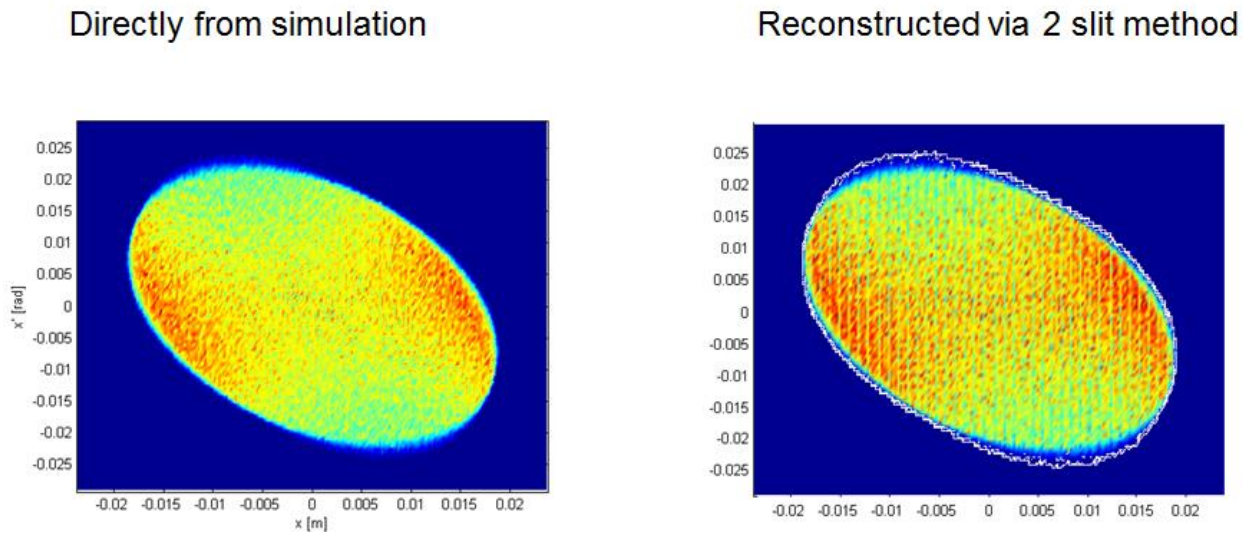

Figure 18: Simulation results of an emittance measurement using the double slit technique.

From our simulations (see Figure 18) we determine that a slit width of 40 μm and separation of 37 cm will result in a 98% accurate emittance measurement.

3.3.3. Round to Flat Transform

Transforming a round magnetized beam to a flat non-magnetized beam requires a beamline of three skew quadrupoles. The magnetized emittance is split into a large and small component by the transformer, as shown in Figure 19. Thus far, simulations have required an additional solenoid to match into the transformer section. Future plans are to find a solution without this magnet for a range of bunch charges.

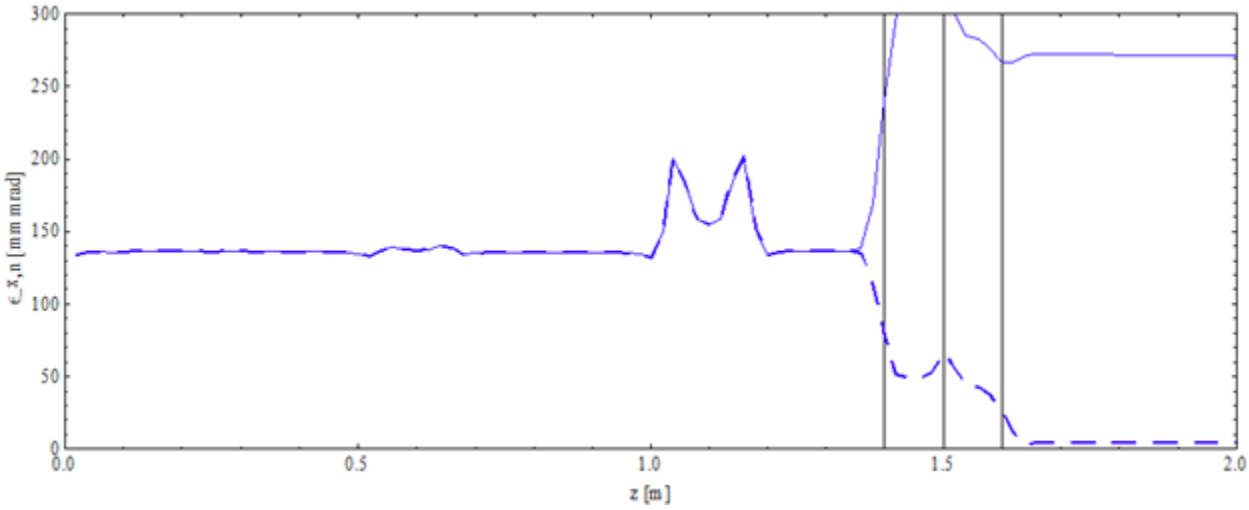

Figure 19: Horizontal and vertical emittance through a round to flat transformer. The vertical lines depict the location of the skew quadrupoles.

4.0 VITA (Lead Scientist)

MATTHEW POELKER
Thomas Jefferson National Accelerator Facility
Newport News, VA 23606

Office Phone: (757) 269-7357
e-mail: poelker@jlab.org
Rank: Senior Staff Scientist
DISCIPLINE: Polarized electrons, Photoelectron guns, Lasers, Vacuum

(a) Professional Preparation

B.S., Engineering Physics, University of Illinois, Champaign/Urbana, IL, December 1983
M.S., Electrical Engineering, Northwestern University, Evanston, IL, June 1988
Ph.D., Electrical Engineering, Northwestern University, Evanston, IL, June 1992
Postdoctoral research associate, Physics Division, Argonne National Lab, January 1992 to May 1994

(b) Appointments

1994-present: Staff Scientist and Group Leader Center for Injectors and Sources, Thomas Jefferson National Accelerator Facility

(c) Recent Journal Publications

1. “Improving the Performance of Stainless-Steel DC High Voltage Photoelectron Gun Cathode Electrodes via Gas Conditioning with Helium or Krypton.” M. BastaniNejad, A. A. Elmustafa, E. Forman, J. Clark, S. Covert, J. Grames, J. Hansknecht, C. Hernandez-Garcia, M. Poelker, R. Suleiman, Nucl. Instr. and Meth. A **762** 135 (2014).
2. “Outgassing Rates of Identical Stainless Steel Chambers Subjected to Different Heat Treatments and with Different Coatings.” M. A. Mamun, P. A. Adderley, M. L. Stutzman, M. Poelker and A. A. Elmustafa, Journal of Vacuum Science and Technology A **32**, 021604 (2014).
3. “Measurement of Electron Beam Polarization from Unstrained GaAs via Two-Photon Photoemission.” J. L. McCarter, A. Afanasev, T. J. Gay, J. Hansknecht, A. Kechiantz, M. Poelker, Nucl. Instr. and Meth. A **738**, 149 (2014).
4. “A search for spin-polarized photoemission from GaAs using light with orbital angular momentum.” N. B. Clayburn, J. L. McCarter, J. M. Dreiling, M. Poelker, D. M. Ryan, T. J. Gay, Phys. Rev. B **87**, 035204 (2013).

(d) Awards

1. E. O. Lawrence Award Recipient, 2011

(e) Committees

1. International Spin Physics Committee since 2012

RIAD SULEIMAN
Jefferson Laboratory, Suite 8
600 Kelvin Dr., Newport News, Virginia 23606
Work: (757) 269-7159
e-mail: suleiman@jlab.org

Employment

- JEFFERSON LABORATORY:
  March 2012 - present. Staff Scientist III, Accelerator Division.
  January 2007 - February 2012. Staff Scientist II, Accelerator Division.
- VIRGINIA POLYTECHNIC INSTITUTE AND STATE UNIVERSITY:
  August 2005 - January 2007. Research Scientist.
  August 2004 - July 2005. Postdoctoral Research Associate.
- MASSACHUSETTS INSTITUTE OF TECHNOLOGY:
  July 2002 - July 2004. Senior Postdoctoral Research Associate at the Laboratory for Nuclear Science.
  October 1999 - June 2002. Postdoctoral Research Associate at the Laboratory for Nuclear Science.

Education

- KENT STATE UNIVERSITY: September 1993 - October 1999.
  Ph.D. student at the Center for Nuclear Research of the Physics Department.
  Doctor of Philosophy degree in Physics awarded in December 1999.
  Thesis project (Adviser: Professor Makis Petratos):
  “Measurement of the Electric and Magnetic Elastic Structure Functions of the Deuteron at Large Momentum Transfers”.
- YARMOUK UNIVERSITY, JORDAN: February 1990 - May 1993.
  Bachelor of Science degree in Physics, 1993.

Professional Affiliation

- American Physical Society

Recent Journal Publications

1. “Measurement of parity violation in electron-quark scattering.” D. Wang et al., Nature 506, **67** (2014).
2. “Charge Lifetime Measurements at High Average Current Using a K_2CsSb Photocathode inside a DC High Voltage Photogun.” R. Mammei, R. Suleiman, et al., Phys. Rev. ST Accel. Beams, **16**, 033401 (2013).
3. “First Determination of the Weak Charge of the Proton.” D. Androic et al., Phys. Rev. Lett. **111**, 141803 (2013).

5.0 Budget Explanation

To be able to perform the proposed measurements, budget is required for the following procurements:

1. Purchase cathode solenoid magnet to provide 2 kG at cathode
2. Three skew quadrupoles to be used as a round-to-flat beam transformer
3. Components installed inside three diagnostics crosses
4. Beamline hardware: steering magnets and slits for beam emittance and magnetization measurements. (note, we have the big ticket items in-house: gun, HV supplies, K_2CsSb preparation chamber, valves, dump, ion pumps, differential pump can and NEG modules, viewer crosses, we have 80/20 aluminum support structure)
5. Laser components
6. postdoc

Work performed outside the gun group will need to be paid for with additional budget:

1. Cathode magnet design and procurement
2. Cathode magnet installation
3. Relocate new CEBAF spare dogleg power supply (500A/80V) and provide 480VAC and LCW
4. Mechanical designer for cathode magnet support
5. Mechanical designer for slits and beamline
6. ASTRA and GPT modeling (Fay Hannon)

The grand total cost for the first year is $339,211 (with overhead). For the second year, the grand total cost is $265,850 (with overhead). For the third year, the grand total cost is $212,025 (with overhead).

6.0 References

1. “Magnetization effects in electron cooling.” Ya. Derbenev and A. Skrinsky, Fiz. Plazmy **4**, 492 (1978) [Sov. J. Plasma Phys. **4**, 273 (1978)].
2. “A low emittance, flat-beam electron source for linear colliders.” R. Brinkmann, Y. Derbenev, and K. Flöttmann, Phys. Rev. ST Accel. Beams **4**, 053501 (2001).
3. “Experimental Demonstration of Relativistic Electron Cooling.” S. Nagaitsev et al., Phys. Rev. Lett. **96**, 044801 (2006).
4. “Cooling of High-Energy Hadron Beams.” M. Blaskiewicz, Annual Review of Nuclear and Particle Science **64**, 299 (2014).
5. “High-energy electron cooling in a collider.” A. V. Fedotov et al., New J. Phys. **8**, 283 (2006).
6. “The TRIUMF-ARIEL RF Modulated Thermionic Electron Source.” F. Ames, Proc. Of EIC’14, Newport News, VA (2014).
7. “Record high-average current from a high-brightness Photoinjector.” B. Dunham et al., Appl. Phys. Lett. **102**, 034105 (2013).
8. “Charge Lifetime Measurements at High Average Current Using a K_2CsSb Photocathode inside a DC High Voltage Photogun.” R. Mammei, R. Suleiman et al., Phys. Rev. ST Accel. Beams **16**, 033401 (2013).
9. “Generation of angular-momentum-dominated electron beams from a Photoinjector.” Y.-E Sun et al., Phys. Rev. ST Accel. Beams **7**, 123501 (2004).
10. “Photoinjector generation of a flat electron beam with transverse emittance ratio of 100.” P. Piot et al., Phys. Rev. ST Accel. Beams **9**, 031001 (2006).
11. “The Advanced Superconducting Test Accelerator (ASTA) at Fermilab: A User-Driven Facility Dedicated to Accelerator Science & Technology.” P. Piot et al., arXiv:1304.0311 [physics.acc-ph] (2013).
12. “Simple algorithm for designing skew-quadrupole cooling configurations.” B. Carlsten and K. Bishofberger, New J. Phys. **8** 286 (2006).
13. “Adapting Optics for High Energy Electron Cooling.” Ya. Derbenev, University of Michigan Report No. UM-HE-98-04 (1998).
14. “Magnet Design for the Magnetized Beam LDRD Proposal.” J. Benesch, Jefferson Lab Tech Note 15-043 (2015).

7.0 Project Milestones

7.1 Year 1 Milestones

- Q1 (Oct, Nov, Dec):
  1. HV condition gun to 350 kV and build K_2CsSb preparation chamber ✓
  2. Design beamline, locate magnets and diagnostics at optimum positions ✓
  3. Design cathode solenoid magnet ✓
- Q2 (Jan, Feb, Mar):
  1. Connect existing beamline to gun and instrument beamline ✓
  2. Procure cathode solenoid magnet ✓
  3. Design and procure slits
- Q3 (Apr, May, Jun):
  1. Commission exiting beamline with beam
  2. Measure photocathode lifetime at 5 mA and 350 kV (not magnetized)
  3. Relocate new spare CEBAF dogleg power supply to GTS
- Q4 (Jul, Aug, Sep):
  1. Install cathode solenoid magnet
  2. Assemble new beamline and commission with beam
  3. Design and procure three skew quads

7.2 Year 2 Milestones

- Q1 (Oct, Nov, Dec):
  1. Generate magnetized beam
  2. Measure mechanical angular momentum vs magnetization and laser size
  3. Benchmark simulation against measurements
- Q2 (Jan, Feb, Mar):
  1. Measure mechanical angular momentum vs bunch charge and bunch length
  2. Benchmark simulation against measurements

- Q3 (Apr, May, Jun):
  1. Generate very high currents magnetized beam and study beam transport vs electron bunch charge

- Q4 (Jul, Aug, Sep):
  1. Measure photocathode lifetime vs magnetization at 5 mA and 350 kV
  2. Study beam halo and beam loss vs magnetization

7.3 Year 3 Milestones

- Q1 (Oct, Nov, Dec):
  1. Install three skew quads
  2. Generate flat beam with skew quads – RTFB Transformer – and measure horizontal and vertical emittances using slit method

- Q2 (Jan, Feb, Mar):
  1. Measure RTFB transformation versus electron bunch charge
  2. Use simulation to quantify how good or complete RTFB transform

- Q3 (Apr, May, Jun):
  1. Change to HV Supply of 32 mA and 200 kV

- Q4 (Jul, Aug, Sep):
  1. Measure photocathode lifetime vs magnetization at 32 mA and 200 kV
  2. Study beam halo and beam loss vs magnetization